BathySAR-Net: An Artificial Neural Network-Based Model For Predicting Intertidal Zone Depth Using Sentinel-1 Synthetic Aperture Radar (SAR) Imagery

Belvana Eka Putri[1], *Muhammad* Aldila Syariz[1,*], *Lino* Garda Denaro[2], and *Manh* Van Nguyen[3]

[1]Geomatics Engineering Department, Sepuluh Nopember Institute of Technology, Surabaya, Indonesia,
[2]National Research and Innovation Agency, Bandung, Indonesia
[3]Faculty of Geography, Hanoi National University of Education, Hanoi, Vietnam

Abstract. Coastal depth monitoring plays a crucial role in navigation and environmental management but is often constrained by the high operational costs and accessibility issues of conventional surveys. To address these challenges, this study implements "BathySAR-Net," an Artificial Neural Network (ANN) model designed to predict sea depth using Sentinel-1 Synthetic Aperture Radar (SAR) imagery combined with BATNAS bathymetric data. The model utilizes a Multilayer Perceptron (MLP) architecture to capture the complex, non-linear relationships between radar backscatter coefficients and water depth. Evaluation using robust K-Fold Cross Validation yielded a Root Mean Square Error (RMSE) of 8.7060 meters and a coefficient of determination (R^2) of 0.0838. While the model demonstrated improved stability in deeper zones (10–15 meters), predictive performance in shallow intertidal areas (<5 meters) remained limited due to significant radar signal noise and data scarcity. These findings suggest that while SAR-based ANN offers a promising, accessible alternative for bathymetry, further integration of hydrodynamic variables is essential to resolve nearshore dynamics effectively.

1. Introduction

Use Coastal zones, serving as a critical transition between terrestrial and marine environments, harbor exceptionally rich ecosystems [1]. These include natural formations such as coral reefs, mangrove forests, estuaries, and deltas, as well as artificial ecosystems like aquaculture ponds, many of which are under threat. However, these natural resources are under intense pressure from anthropogenic activities, such as overfishing driven by market demand, which often involves destructive practices [2]. Concurrently, the impacts of global climate change are a major contributing factor to abrasion and erosion, which significantly alter bathymetric contours and threaten the stability of coastal aquatic ecosystems [3].

* Corresponding author: aldilasyariz@its.ac.id

Monitoring bathymetric changes is therefore a crucial step for understanding coastal environmental dynamics [4]. Historically, these measurements have been conducted using two primary approaches: direct methods, such as diver surveys and lead-lines, and indirect methods that rely on advanced acoustic instruments like Single Beam Echosounder (SBES) and Multi Beam Echosounder (MBES) [5]. While capable of yielding high-accuracy data, the field application of these methods is largely inefficient. They are time-consuming, expensive, highly dependent on favorable weather conditions, and require extensive expert teams [6]. These constraints are exacerbated in shallow intertidal zones, where the accessibility of survey vessels is severely limited by their draft, precluding safe and optimal operation.

To overcome these limitations, remote sensing technology offers an alternative that enables large-scale bathymetric mapping without direct physical contact with the target [7]. Within the field of remote sensing, satellite imagery from active sensors, such as Synthetic Aperture Radar (SAR), demonstrates superior potential over passive sensors, which are dependent on solar illumination. The fundamental advantage of SAR lies in its ability to emit its own microwave pulses and record the backscatter, enabling effective operation regardless of cloud cover, fog, or darkness [8]. Consequently, data from satellites such as Sentinel-1 SAR are ideal for monitoring highly dynamic and constantly changing intertidal zones.

Although SAR technology consistently provides surface data, interpreting the radar backscatter signal to determine water depth is not a straightforward task. The relationship between radar signal characteristics and water depth is highly complex and non-linear, influenced by multiple factors including sea surface roughness and seabed material composition [9]. Addressing this challenge requires an analytical method capable of identifying hidden patterns within the data. This study proposes the use of an Artificial Neural Network (ANN), a machine learning method inspired by the information processing capabilities of the human brain [10]. By training on a given dataset, an ANN model can learn to approximate these non-linear relationships autonomously [11]. Therefore, the objective of this research is to develop and evaluate the performance of an ANN model for predicting intertidal zone depth along the coast of Bawean Island, Gresik, using Sentinel-1 SAR data. The model's accuracy will be quantitatively assessed using the Root Mean Square Error (RMSE) and the Coefficient of Determination (R^2)

2. Materials and Methods

2.1 Study Area & Datasets

This research was conducted on Bawean Island, which is administratively part of Gresik Regency, East Java, and located in the Java Sea. The specific study area is defined by the

coordinates 5°49’4.8” to 5°50’27.6” South latitude and 112°44’2.4” to 112°46’1.2” East longitude.

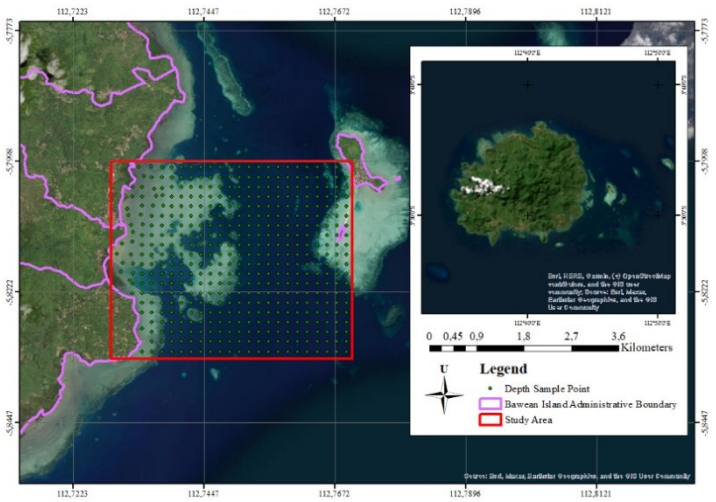

Fig. 1. Map of the study area

The southern coastal region of Bawean Island encompasses diverse habitats, including sandy, vegetated, and rocky shores, supported by critical ecosystems such as mangrove forests, seagrass beds, and coral reefs. However, these ecosystems face significant pressure from anthropogenic activities, including illegal logging and destructive fishing practices, leading to reduced coverage of coral reefs, mangroves, and seagrass. Oceanographically, the area is influenced by ocean waves with an average height of 1.41 meters and exhibits a diurnal tidal pattern. While the coastal abrasion rate is relatively low, at approximately 0.5 meters per year, the impacts of sea-level rise—such as coastal flooding (locally known as *rob*) and saltwater intrusion—are already affecting the local community [12].

The dataset consists of Sentinel-1A SAR imagery acquired on 29 May 2021 at 10:50 (UTC+7) in Interferometric Wide Swath mode with VV and VH polarizations, ascending orbit. The imagery was obtained from the Copernicus Open Access Hub. Bathymetric data were derived from the National Bathymetric Chart (BATNAS) produced by the Geospatial Information Agency (BIG) through the integration of gravity anomaly inversion and sounding data from multiple institutions. The dataset covers 110–115° E and 10–5° S at a spatial resolution of 6 arc-seconds (±180 m) referenced to the Mean Sea Level (MSL) datum, and was accessed via Ina-Geoportal.

2.2 Methodology

The research workflow commences with the acquisition of Sentinel-1 Ground Range Detected (GRD) SAR imagery and the National Bathymetry (BATNAS) dataset. This is followed by the extraction of depth soundings from the BATNAS data and a comprehensive pre-processing pipeline for the SAR imagery. The pre-processing stage yields calibrated backscatter values ($\beta°, \gamma°, \sigma°$) for both VV and VH polarizations. These two datasets are then

merged, normalized, and labelled. To ensure a robust model evaluation, a 10-Fold Cross-Validation scheme is implemented. The prepared data is used to train and validate the proposed BathySAR-Net (Artificial Neural Network) architecture. Finally, the trained model is employed for depth prediction across the study area, with the final output presented as a bathymetric map.

2.2.1 Data Pre-Processing

The primary dataset utilized in this study is the Sentinel-1 Level-1 Ground Range Detected (GRD) Synthetic Aperture Radar (SAR) imagery. This dataset was selected due to its high spatial resolution and its ability to acquire data independently of weather conditions and daylight availability. The preprocessing stage is essential to enhance the quality of the SAR imagery and prepare it for further analysis. The preprocessing workflow begins with subsetting, which limits the analysis to the specific study area. This is followed by the Apply Orbit File process, which corrects the satellite's positional accuracy by incorporating updated orbital information from the metadata. Next, Thermal Noise Removal is conducted to eliminate thermal noise artifacts that can interfere with the backscatter signal, thereby improving the reliability of the image. The Border Noise Removal step follows, which removes noise along the image edges and filters out invalid pixels. Subsequently, Radiometric Calibration is applied to convert Digital Number (DN) values into calibrated backscatter coefficients, expressed as sigma naught (σ^0), in decibel (dB) units. This step ensures that the backscatter values are physically meaningful and comparable across different scenes. Speckle Filtering is then performed to reduce speckle noise, a common granular noise in SAR data, thereby enhancing image clarity. Following this, Range Doppler Terrain Correction is implemented to rectify geometric distortions caused by topographic variation and sensor geometry. The output of this preprocessing stage includes sigma naught values and incidence angle data, which are essential for subsequent feature extraction. The final preprocessing step is the conversion to decibels (dB), which transforms the calibrated backscatter values into logarithmic scale to facilitate interpretation and analysis [13]. After completing the SAR preprocessing workflow, the next phase involves extracting depth information from the BATNAS bathymetric dataset within the study area. This process yields 429 spatially distributed depth data points, ranging from 0 to 32 meters. Following the integration of SAR-derived features and depth labels from BATNAS, the dataset undergoes a data preparation stage prior to model training. This includes data normalization using the Min-Max Scaling method, which serves to standardize the range of all input features. This normalization ensures that variables with larger value ranges do not disproportionately influence the learning process [14]. Min-Max Scaling transforms each feature value into a new scale—typically between 0 and 1—according to the following formula:

$$x' = \frac{x - \min}{\max - \min} \tag{1}$$

where x' is the normalized value, x is the original data value, and *min* and *max* represent the original minimum and maximum values, respectively. Once all feature values have been normalized, the prepared dataset is validated using a 10-Fold Cross Validation scheme. In this method, the dataset is divided into ten equally sized subsets or "folds." The training and validation process is performed iteratively ten times, where in each iteration, one fold is used as the validation set while the remaining nine folds are used for training. This technique ensures that each data point is used exactly once for validation and nine times for training.

As a result, this approach provides a more robust and unbiased estimate of model performance by minimizing the variability caused by any single train-test split.

2.2.2 BathySAR-Net Network Structure

In this study, the proposed Artificial Neural Network (ANN) model is referred to as BathySAR-Net. This model is developed using a Multilayer Perceptron (MLP) architecture implemented with the Keras Sequential API, specifically designed to learn the non-linear relationship between backscatter coefficients derived from Synthetic Aperture Radar (SAR) data and corresponding water depth values. The selection of input features is grounded in the hydrodynamic modulation theory of SAR bathymetry. Since microwave radar cannot penetrate the water column, depth estimation relies on the indirect imaging mechanism where underwater topography modulates the surface current velocity. This interaction alters the sea surface roughness, which in turn modifies the radar backscatter intensity through Bragg resonance [15]. To capture these nuances, the model incorporates Sigma Nought ($\sigma°$) as the primary indicator of surface roughness, alongside Beta Nought ($\beta°$) and Gamma Nought ($\gamma°$) to account for radar reflectivity and geometric incidence angle corrections. Both VV and VH polarizations are utilized to distinguish between surface scattering (VV-dominant) and volume scattering or noise (VH-dominant). Therefore, the model input consists of six discrete features: $\beta°$ VH, $\beta°$ VV, $\gamma°$ VH, $\gamma°$ VV, $\sigma°$ VH, and $\sigma°$ VV.

The network architecture is configured with a single hidden layer containing 64 neurons, followed by an output layer consisting of a single neuron responsible for predicting the water depth value directly. The model was trained using the Adam optimizer with a learning rate of 0.001, minimizing the Mean Squared Error (MSE) loss function. Training was conducted for a maximum of 300 epochs with a batch size of 64. To prevent overfitting and enhance generalization, three regularization techniques were applied. First, the ReLU activation function was used in the hidden layer, followed by a Dropout layer with a rate of 0.3, meaning that 30% of neurons were randomly deactivated at each training step. Second, L2 regularization with a lambda coefficient of 0.01 was implemented to control model complexity. Third, an Early Stopping mechanism with a patience value of 20 was employed to automatically halt training if no improvement was observed in validation performance for 20 consecutive epochs. The final performance of the model was evaluated using the Root Mean Squared Error (RMSE) metric to assess the accuracy of depth predictions.

2.2.3 Performance Evaluation of BathySAR-Net

To evaluate the predictive performance of the proposed ANN model, this study employs two primary statistical metrics: Root Mean Squared Error (RMSE) and the Coefficient of Determination (R^2). These metrics are selected for their ability to provide a comprehensive assessment of model accuracy and explanatory power. RMSE is particularly useful because it quantifies the average magnitude of prediction error in the same units as the target variable (i.e., depth in meters), making the results intuitive and easy to interpret. A lower RMSE value indicates better predictive accuracy.In contrast, R^2 complements the evaluation by indicating the proportion of variance in the observed depth values that is explained by the model. An R^2 value closer to 1 signifies a strong correlation between the predicted and actual values, suggesting a well-fitted model. The RMSE is calculated using the following formula:

$$RMSE = \sqrt{\frac{1}{n}\sum_{i=1}^{n}(yi - \hat{y}\imath)^2} \quad (2)$$

where n is the total number of data points, y_i is the actual depth value, and $\hat{y}_i$ is the depth value predicted by the model. The Coefficient of Determination (R^2) is calculated by comparing the sum of squared residuals to the total sum of squares, using the following formula:

$$R^2 = \frac{SSR}{SST} = \frac{\sum_{i=1}^{n}(\hat{y}\imath - \bar{y})^2}{\sum_{i=1}^{n}(yi - \bar{y})^2} \quad (3)$$

In this formula, $\hat{y}_i$ is the predicted value, y_i is the actual value, and $\bar{y}$ is the mean of all actual depth values.

3. Results

To evaluate the performance of the ANN model in estimating sea depth, this research conducted testing using the 10-Fold Cross-Validation method on the BathySAR-Net model as an initial case study. The results from each fold were recorded to observe the variability of the model's performance against the data division. The evaluation metrics used are Root Mean Squared Error (RMSE) and R-squared (R^2). RMSE provides information regarding the average magnitude of prediction error in meters, which in this research represents the deviation of the predicted depth from the actual value. Meanwhile R^2 indicates the proportion of variance in the depth data that can be explained by the model, with a higher value indicating a better fit of the model to the observation data. The following is a statistical visualization of the depth distribution for each fold:

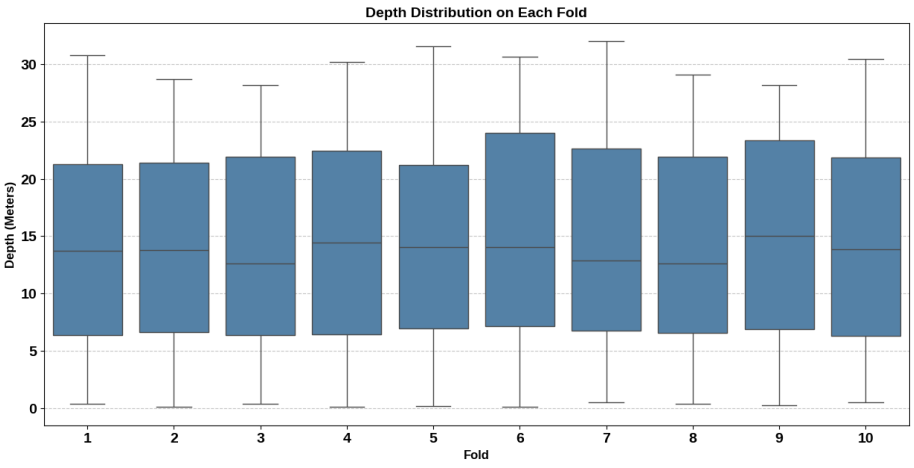

Fig. 2. Depth Distribution on Each Fold

Statistical analysis of depth distribution in each fold indicates that the data partitioning in the 10-fold cross-validation was conducted in a representative and balanced manner. The mean depth for each fold ranged from 14.019 meters to 14.779 meters, with a maximum difference of only 0.760 meters, reflecting equality in central tendency. The median depth was also consistent, ranging from 12.619 meters to 15.016 meters, indicating stability in the central value. The standard deviation, as an indicator of data dispersion, exhibited a uniform pattern across all folds, ranging from 8.800 meters to 9.244 meters with a difference of only 0.444 meters. Depth ranges were similarly consistent, with minimum values approaching 0 meters in all folds and maximum values varying from 28.149 meters to 32.009 meters. Although Fold 3 and Fold 8 displayed slightly lower medians (around 12.6 meters) and Fold 9 showed a more concentrated data distribution with the highest median, lowest standard deviation, and lowest maximum value, these variations are minor and statistically insignificant. Overall, this uniform distribution provides a fair and robust foundation for evaluating the ANN model's performance. This consistency ensures that evaluation results can be interpreted objectively, as they are influenced purely by the model architecture's performance rather than imbalances in data distribution.

To assess the performance of the BathySAR-Net model for identifying sea depth, this research employed a Multilayer Perceptron (MLP) architecture configured with a single hidden layer containing 64 neurons. This architecture was designed to efficiently capture the non-linear relationship between the six input features— β° VV+VH, γ° VV+VH, and σ°VV+VH —and the single output value representing depth. The training process for the model employed an identical set of optimized hyperparameters, including activation function, optimizer, and learning rate, to ensure robust and stable learning. The final performance of the BathySAR-Net model was quantitatively assessed using the average RMSE and R^2 values obtained from the 10-Fold Cross-Validation, as presented in Table 1.

Table 1. Visualization of ANN Model Architectures

Model	RMSE (m)	R^2 (m)
BathySAR-Net (64 Neurons)	8.7060	0.0838

Based on the 10-Fold Cross-Validation, the BathySAR-Net model demonstrated a Root Mean Squared Error (RMSE) of 8.7060 meters and a coefficient of determination (R^2) of 0.0838. The RMSE value indicates that, on average, the model's depth estimation deviates by approximately 8.7 meters from the actual depth value. Furthermore, the low R^2 value suggests that the model only explains a small proportion of the total variance in the observed depth data. This outcome, despite the consistent training process, indicates that the model's performance is primarily constrained by the limited information content in the input features (Sentinel-1 backscatter values). This suggests that the relationship between the radar backscatter and depth, as captured by this particular set of features, does not substantially dominate the variance in the depth data. BathySAR-Net Model was therefore employed in the subsequent stage to generate bathymetric predictions for the study area, as illustrated in Figure 3.

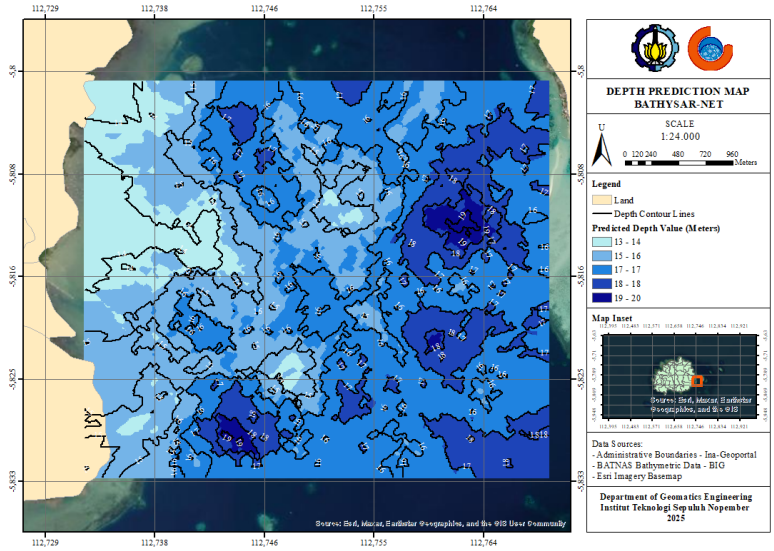

Fig. 3. Predicted Bathymetry Map using the BathySAR-Net Model

The predicted bathymetry map reveals a diverse depth distribution, ranging from shallow waters of approximately 13 meters, represented in light blue, to depths exceeding 19 meters, shown in dark blue. Spatially, deeper areas are consistently located in the southeastern part of the study area, extending toward the northeast, while shallower waters dominate the western and northern regions adjacent to Bawean Island's coastline. From a seafloor morphology perspective, the tightly spaced contours in the southeast indicate steep slopes, likely representing submarine escarpments where depth changes occur rapidly. In contrast, the wider contour spacing in the west and north suggests a gently sloping and relatively flat seabed. The presence of dark blue to purple areas in the southeast further suggests possible geomorphological features such as localized depressions or small troughs. These patterns appear consistent rather than random, indicating the potential presence of significant underwater structures that could be subjects of further investigation.

However, as this map is the output of an ANN-based model derived from radar imagery, it is important to note that the spatial patterns strongly depend on the quality and spatial resolution of the input data. In areas with noise or unrepresentative SAR texture—caused, for instance, by high waves or exceptionally calm sea surfaces—the model may produce less accurate predictions. Therefore, field verification remains essential to confirm the identified geomorphological features.

4. Discussion

This section presents an in-depth analysis of predicted depth variations compared with actual depths across the ranges of 0–5 meters, 0–10 meters, 0–15 meters, and 0–20 meters, as discussed in Section 4.1, followed by the application of the model to a different water area in Section 4.2.

4.1 Comparative Analysis of Predicted and Actual Depths Across Depth Ranges

To evaluate the model's performance in predicting bathymetry across different depth ranges, visualizations were generated for 0–5 meters, 0–10 meters, 0–15 meters, and 0–20 meters. This analysis aimed to specifically assess the model's ability to represent varying depth levels, particularly in shallow waters, which are generally more sensitive to variations in radar signals. The visualizations compare actual depth data from BATNAS with the model's predictions for each range. By progressively limiting the depth intervals, this approach provides a more detailed understanding of the model's spatial accuracy and predictive value distribution, while also identifying potential biases or error patterns at specific depths. The following figures present the visualization results for each depth range, illustrating spatial comparisons between actual data and the ANN model's bathymetric predictions.

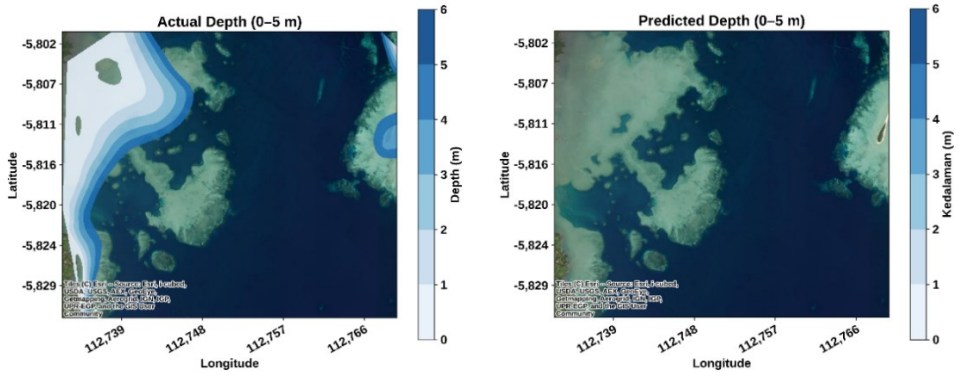

Fig. 4. Comparison of Actual and Predicted Depth Visualizations for the 0–5 Meter Range

In the first depth range (0–5 meters), the ANN model failed to produce any predictions, as indicated by the absence of depth values in the visualization. This is a critical issue, considering that this very shallow zone corresponds to the intertidal area, which is a primary focus of the study.

The results suggest that the model was unable to recognize SAR backscatter patterns representative of extremely shallow waters. This critical limitation in the 0-5 m range is primarily attributed to the physical complexity of the intertidal zone and data scarcity, rather than the ANN architecture itself. Physically, the intertidal zone is a highly dynamic environment characterized by breaking waves, extreme surface turbulence, and rapid tidal fluctuations. In these conditions, the radar backscatter is dominated by non-coherent noise and specular reflections from exposed seabeds during low tide, which mask the subtle hydrodynamic modulation required for bathymetric extraction. Furthermore, the training dataset contained a disproportionately low number of samples for the 0-2 m range, preventing the model from learning a stable representation of these chaotic signal patterns. Consequently, this study suggests that for operational intertidal mapping, the proposed SAR-based method cannot be used as a standalone solution and requires integration with auxiliary data, such as tidal gauges or optical imagery, to resolve nearshore ambiguities.

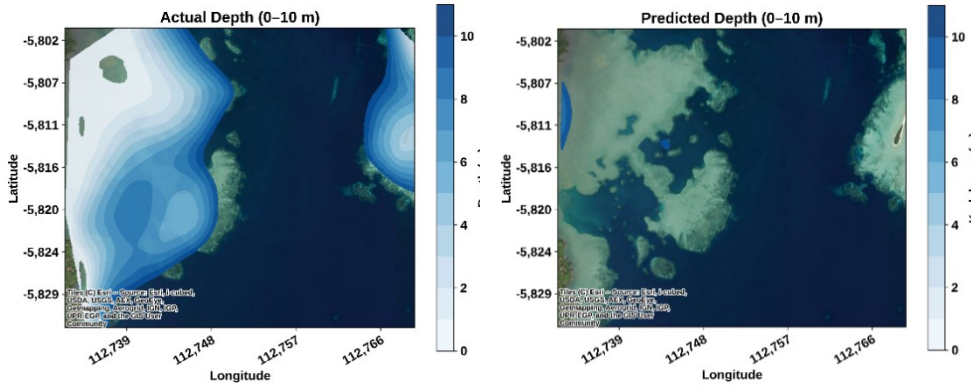

Fig. 5. Comparison of Actual and Predicted Depth Visualizations for the 0–10 Meter Range

The figure above compares actual depth maps and ANN model predictions for the 0–10 m range. Overall, the ANN model shows limitations in mapping shallow waters, especially within and around the intertidal zone. Two key observations can be made. First, in the actual depth map, the northwestern and southwestern intertidal areas display a broad, well-defined 0–5 m contour zone, while in the predicted map these areas are poorly detected, with only small portions classified within the correct range. Second, predicted depths are scattered irregularly without forming clear contour patterns, as seen in the central part of the map, where depths of 8–10 m are predicted in areas that are actually shallower or outside the 0–10 m range.

Spatial inconsistencies are also apparent where areas with uniform actual depths contain prediction anomalies or artifacts. These issues indicate the model's difficulty in capturing the spatial and textural relationships in shallow-water backscatter data. Likely causes include:

1. High environmental dynamics in the intertidal zone, such as substrate variability, tides, and shallow-wave effects influencing backscatter.
2. Limited training data for very shallow depths (0–2 m), reducing the model's ability to distinguish relevant signals.
3. The ANN's current architecture being less effective at extracting spatial features for shallow depths, performing better for deeper, more stable patterns.

Improving performance in this zone may require adding shallow-water training samples and enhancing the model architecture or integrating additional features such as texture indices or tidal data.

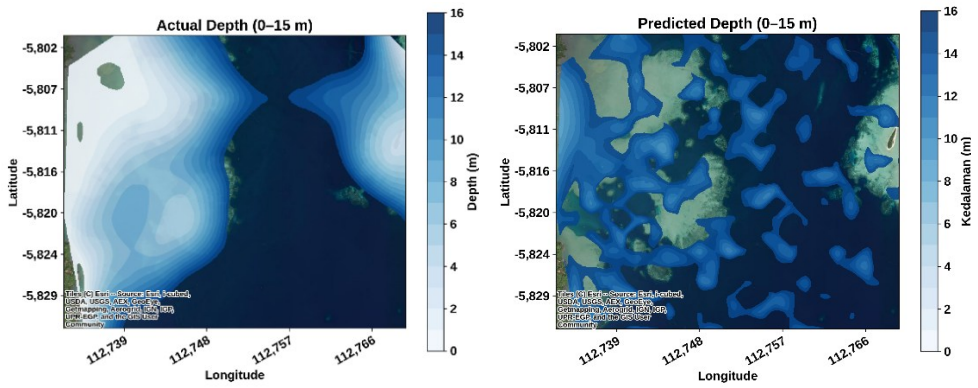

Fig. 6. Comparison of Actual and Predicted Depth Visualizations for the 0–15 Meter Range

The visualization above compares the actual depth map with the ANN model's predicted depth map for the 0–15 m range. Compared to the 0–10 m range, the ANN model demonstrates a broader spatial coverage in its predictions. However, several notable limitations remain in its performance.

A major issue lies in the misclassification of shallow-water areas. Several regions with depths of less than 5 m in the actual data are predicted to fall within the 10–16 m range, visually represented by dark blue contours near the shoreline. The distribution of these predictions also appears spatially inconsistent, with similar depth values scattered in non-adjacent locations and failing to form natural contour patterns. This indicates a tendency toward overestimation in shallow zones, likely due to the model's difficulty in distinguishing SAR backscatter signals for shallow to intermediate depths.

In the central and northeastern portions of the prediction map, areas of high predicted depth appear in locations that do not match the smooth depth gradient observed in the actual map. This suggests that the model has not fully captured the spatial transitions of depth across the study area.Potential contributing factors to these errors include:

1. An imbalance in training data representation between shallow and intermediate depths.
2. The complexity of SAR backscatter reflectance in mixed-substrate environments (sand, mud, submerged vegetation), which is challenging for conventional ANN models to differentiate.
3. The model's limited ability to incorporate spatial context between neighboring pixels, resulting in fragmented depth patterns.

While the predictions for this range show improved spatial coverage compared to the 0–10 m case, accuracy in separating shallow and intermediate depths remains an area for improvement.

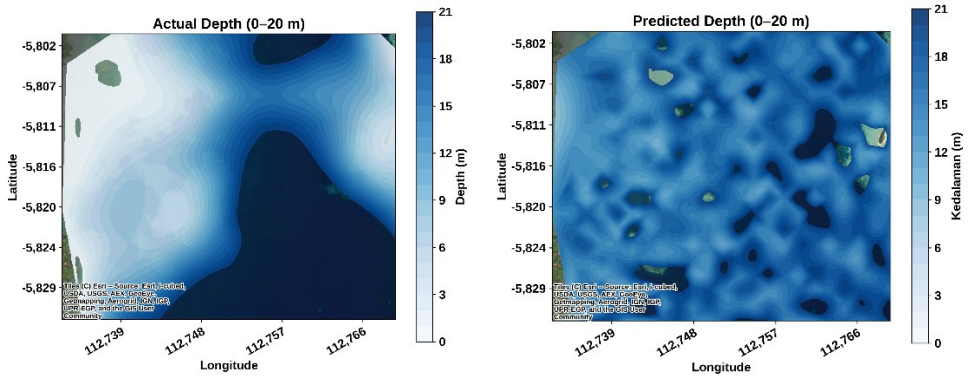

Fig. 7. Comparison of Actual and Predicted Depth Visualizations for the 0–20 Meter Range

A closer examination of the two maps reveals stark differences in how depth is distributed. The actual depth map displays smooth and orderly contour gradients, with depth increasing gradually from the shoreline toward the open sea. This pattern aligns with the typical morphology of coastal seabeds, which generally feature gentle slopes and consistent contour lines. In contrast, the predicted map exhibits irregular and fragmented depth patterns, with random spatial distributions that fail to reflect natural contour gradients. Areas of high (dark) and low (light) depth values appear scattered without a coherent spatial structure.

The mismatch becomes even more evident when examining the shallow-depth patterns in the predicted map. Numerous low-depth patches (0–6 m) appear inconsistently within regions that should be considerably deeper (10–20 m). Such patterns suggest potential local overfitting or noise during model training, where the ANN captures non-representative variations in the training data. The presence of artifact-like spots further indicates that the model struggles to capture spatially coherent depth patterns.

This spatial inconsistency points to a fundamental weakness in the model's ability to recognize the natural structure of seafloor contours. Compared to actual conditions, the ANN's predictions fail to capture continuous bathymetric structures, revealing its limited capacity to generalize in areas underrepresented in the training set. This lack of generalization poses a major challenge for applying ANN-based SAR imagery to bathymetric prediction.

Possible factors contributing to the poor predictive accuracy for this depth range include:

- The absence of explicit spatial features in the model's input (the ANN processes individual pixel values without accounting for spatial relationships between pixels).
- The increasing complexity of SAR backscatter signals at depths >10 m due to radar energy attenuation.
- Imbalanced training data distribution, particularly in the mid-depth (10–15 m) and deep (15–20 m) classes, causing prediction bias toward certain depth categories.

These findings indicate that, although the ANN model's predictions cover the full extent of the study area, the accuracy of its bathymetric representation remains low. Further steps are

needed to enhance prediction accuracy, including data augmentation, outlier filtering and spatial smoothing, and integration with spatially-aware models.

Synthesizing the performance across all depth ranges, the overall low coefficient of determination ($R^2 = 0.0838$) warrants a fundamental physical explanation. Unlike optical bathymetry methods, which directly measure light attenuation through the water column and typically achieve higher correlations ($R^2 > 0.7$) in clear waters, SAR bathymetry relies on an indirect imaging mechanism. The radar signal does not penetrate the water; instead, it captures the modulation of sea surface roughness induced by the interaction between tidal currents and underwater topography. The results of this study suggest that relying solely on backscatter intensity features (σ^0) without explicit hydrodynamic input data (e.g., current velocity) limits the model's explanatory power to resolve this complex, indirect relationship. Consequently, the primary scientific contribution of this work is in delineating the performance boundaries of pure backscatter-based ANN models, highlighting that machine learning architectures alone cannot fully compensate for the lack of hydrodynamic variables in SAR bathymetry.

4.2 Application of the Model to a Different Coastal Area

As part of the extended analysis of BathySAR-Net's performance, an additional prediction test was conducted using Sentinel-1 SAR imagery from a location situated near the previous study area, but slightly shifted to the south. The objective of this test was to evaluate the model's ability to generalize across both familiar areas (previously included in training) and new, unseen regions. The dataset used for this evaluation was derived from Sentinel-1 SAR imagery of the Bawean Island region, acquired in May 2025. The imagery underwent the same pre-processing steps as the 2021 dataset used for model training, ensuring consistency in input preparation and comparability of results. The following figure presents the predicted bathymetry map generated by BathySAR-Net based on the newly acquired imagery.

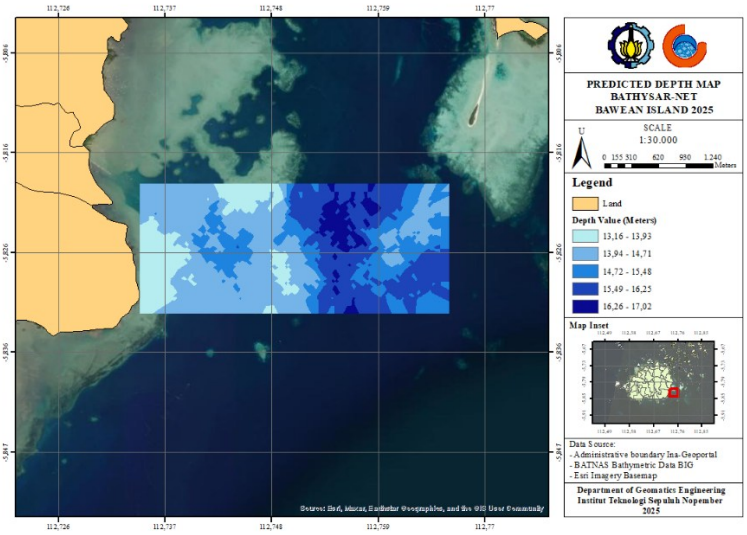

Fig. 8. Predicted Bathymetry of Bawean Island (2025)

To facilitate evaluation, the predicted bathymetric values generated by the model were grouped into five depth ranges: 0–5 m, 5–10 m, 10–15 m, 15–20 m, and >20 m. Accuracy assessment was then carried out for each range using two primary metrics: the Root Mean Square Error (RMSE), which measures the absolute prediction error, and the relative RMSE, calculated by comparing the RMSE value to the maximum depth of each range. This approach was adopted because each range has a different depth span, making the interpretation of error values more proportional. In other words, the same absolute error may have a different impact depending on the maximum depth of the range. The model's performance evaluation results for each depth range are presented in Table 2.

Table 2. RMSE Values Across Depth Ranges for the BathySAR-Net Model (2025)

Depth Range	RMSE (m)	Relative RMSE (%)	Number of Data Points
0 – 5	11,652	389,66	9
5 – 10	7,249	102,90	41
10 – 15	2,830	22,67	14
15 – 20	4,025	22,65	20
> 20	11,154	42,83	93

The highest RMSE value was observed in the 0–5 m depth range, both in absolute terms (11.652 m) and relative terms (389.66%). This high percentage error occurs because the maximum depth in this range is only about 5 m, meaning that even a small deviation of a few meters in prediction can result in a disproportionately large relative error. This substantial inaccuracy is likely due to the complex characteristics of shallow waters, such as tidal influence, wave disturbances, turbidity changes, and specular reflections from the water surface, which introduce significant noise into the SAR backscatter signal.

Model performance improves slightly in the 5–10 m range; however, the relative RMSE remains high at 102.9%. This indicates that the intertidal to shallow subtidal zones remain a significant challenge for SAR-based bathymetry modeling, particularly because radar imagery has limited penetration through the water column and is more sensitive to surface conditions.

In contrast, model performance improves considerably in the 10–15 m and 15–20 m depth ranges, with relative RMSE values around 22%. This suggests that the model begins to effectively learn and identify patterns linking SAR backscatter values to water depth in these mid-depth zones. At these depths, SAR imagery tends to exhibit more stable backscatter values and is less affected by surface dynamics, allowing the model to generalize more effectively.

In the >20 m depth range, the absolute RMSE increases again to 11.154 m, yet the relative RMSE remains at a moderate 42.83% due to the larger scale of depth values in this range. In other words, while the absolute error is substantial, it is proportionally more acceptable for deep-water estimation. Moreover, this range contains the largest number of evaluation points (93), making the performance assessment more representative.

Spatially, the predicted results are visualized as a depth distribution map classified into five ranges. Light blue represents shallow areas, while dark blue denotes deeper waters. The visual pattern shows that the eastern and southeastern parts of Bawean Island are dominated by greater depths, which is consistent with the seafloor topography indicated in previous bathymetric maps.

Although the final visualization does not yet exhibit smooth and detailed depth contours comparable to interpolated conventional bathymetric surveys, the model successfully produces a logical depth distribution pattern and spatial depth gradient. This is evident from the consistent transition of colors from shallow to deep zones, albeit still in coarse segmented blocks rather than continuous contours. Such visual coarseness may be attributed to:

- Limited observation points in certain ranges, resulting in suboptimal spatial interpolation.
- High local variability not fully captured by the model due to SAR's spatial resolution limitations or inherent data noise.

While limitations persist, particularly in shallow-water zones, these results demonstrate that BathySAR-Net has promising potential as an alternative approach for bathymetric mapping using SAR imagery. The model's ability to predict logical depth patterns in mid- to deep-water zones suggests it could be operationally viable, especially in areas difficult to access with conventional bathymetric surveys. Future model development could focus on expanding the quantity and diversity of training data, integrating tidal corrections, implementing spatial models such as CNNs, and conducting temporal and cross-location validation to ensure stronger generalization.

Overall, BathySAR-Net's predictions for 2025 Sentinel-1 SAR imagery of Bawean Island indicate a reasonably good generalization capability in mid- and deep-water depths, although performance in shallow zones still requires improvement. The spatial visualizations suggest that the model is beginning to capture realistic depth patterns, albeit with coarse contours. With further development and improved data quality, this approach could serve as an efficient alternative for radar-based bathymetric mapping.

5. Conclusion

Based on the findings and discussions presented in the previous chapters, it can be concluded that the BathySAR-Net model, which utilizes a Multilayer Perceptron (MLP) with a single hidden layer and 64 neurons, still falls short of practical applicability, particularly in shallow waters or intertidal zones. Despite undergoing systematic training and evaluation, the model achieved an average Root Mean Squared Error (RMSE) of 8.7060 meters with a coefficient of determination (R^2) of only 0.0838, indicating a very weak correlation between predicted and actual depths. Performance was notably uneven across depth ranges, with the model performing best at depths greater than 20 meters (RMSE: 4.061 meters) but failing to accurately predict depths below approximately 11 meters. While performance improved slightly when tested across a broader depth range with more data—where RMSE increased to 11.729 meters—the inability to capture the characteristics of intertidal zones remained a major limitation. This result suggests that for SAR backscatter data, which typically exhibits weak signals and high noise, the chosen MLP architecture provides the most effective balance, as overly complex models are more prone to overfitting by learning noise rather than meaningful patterns. This performance gap is primarily attributed to the physical limitations of the SAR backscatter signal itself, which has an inherently weak and non-linear relationship with water depth. To address this limitation and enhance predictive performance in future

developments, it is recommended to integrate external environmental data, such as wind speed and ocean currents, into the modeling process. Since SAR backscatter is fundamentally modulated by sea surface roughness, incorporating these hydrodynamic variables could significantly strengthen the model's ability to distinguish between depth-induced patterns and surface noise caused by environmental dynamics.

Acknowledgment
The authors would like to express their sincere gratitude to the European Space Agency (ESA) for providing access to the Sentinel-1 imagery, and to the Geospatial Information Agency of Indonesia (Badan Informasi Geospasial, BIG) for supplying the tidal observation data in the vicinity of Bawean Island. These datasets were essential for the implementation and validation of this study.

Conflict of Interest
The authors declare no conflict of interest.

References

[1] S. A. Mukhtar, G. Handoyo, and H. Setiyono, “Studi Batimetri Dan Pasang Surut Untuk Rekomendasi Alur Pelayaran Di Dermaga Pelabuhan Marunda,” *Indones. J. Oceanogr.*, vol. 6, no. 4, pp. 375–382, 2024, doi: 10.14710/ijoce.v6i4.16541.

[2] M. Postacchini and A. Romano, “Dynamics of the Coastal Zone,” *J. Mar. Sci. Eng.*, vol. 7, no. 12, pp. 7–9, 2019, doi: 10.3390/jmse7120451.

[3] Z. A. Khamis, R. Kalliola, and N. Käyhkö, “Geographical characterization of the Zanzibar coastal zone and its management perspectives,” *Ocean Coast. Manag.*, vol. 149, pp. 116–134, 2017, doi: 10.1016/j.ocecoaman.2017.10.003.

[4] R. Bishop-Taylor, S. Sagar, L. Lymburner, and R. J. Beaman, “Between the tides: Modelling the elevation of Australia’s exposed intertidal zone at continental scale,” *Estuar. Coast. Shelf Sci.*, vol. 223, no. March, pp. 115–128, 2019, doi: 10.1016/j.ecss.2019.03.006.

[5] Osayi Philip Igbinenikaro, Oladipo Olugbenga Adekoya, and Emmanuel Augustine Etukudoh, “Review of Modern Bathymetric Survey Techniques and Their Impact on Offshore Energy Development,” *Eng. Sci. Technol. J.*, vol. 5, no. 4, pp. 1281–1302, 2024, doi: 10.51594/estj.v5i4.1018.

[6] P. Westfeld, H. G. Maas, K. Richter, and R. Weiß, “Analysis and correction of ocean wave pattern induced systematic coordinate errors in airborne LiDAR bathymetry,” *ISPRS J. Photogramm. Remote Sens.*, vol. 128, pp. 314–325, 2017, doi: 10.1016/j.isprsjprs.2017.04.008.

[7] M. Ellis, R. Formanek, and N. Townsend, “Satellite Derived Bathymetry AusSeabed Community Guidelines: Satellite Derived Bathymetry,” p. 13, 2022.

[8] H. Cruz, M. Véstias, J. Monteiro, H. Neto, and R. P. Duarte, “A Review of Synthetic-Aperture Radar Image Formation Algorithms and Implementations: A Computational Perspective,” *Remote Sens.*, vol. 14, no. 5, pp. 1–30, 2022, doi: 10.3390/rs14051258.

[9] R. M. Asiyabi, A. Ghorbanian, S. N. Tameh, M. Amani, S. Jin, and A. Mohammadzadeh, "Synthetic Aperture Radar (SAR) for Ocean: A Review," *IEEE J. Sel. Top. Appl. Earth Obs. Remote Sens.*, vol. 16, pp. 9106–9138, 2023, doi: 10.1109/JSTARS.2023.3310363.

[10] T. Sagawa, Y. Yamashita, T. Okumura, and T. Yamanokuchi, "Shallow Water Bathymetry Derived by Machine Learning and Multitemporal Satellite Images," *Int. Geosci. Remote Sens. Symp.*, pp. 8222–8225, 2019, doi: 10.1109/IGARSS.2019.8899043.

[11] D. Ushizima, *Artificial neural networks*. 2023. doi: 10.1201/9781003359593-7.

[12] Z. Hidayah, A. Romadhon, and Y. Witjarnoko, "Penilaian Kerentanan Wilayah Pesisir Selatan Pulau Bawean terhadap Kenaikan Muka Air Laut Vulnerability Analysis of Sea Level Rise In The Southern Coast of Bawean Island," vol. 20, no. 2, pp. 87–94, 2018, doi: 10.22146/jfs.36109.

[13] F. Filipponi, "Sentinel-1 GRD Preprocessing Workflow," p. 11, 2019, doi: 10.3390/ecrs-3-06201.

[14] Y.-S. Kim, M. K. Kim, N. Fu, J. Liu, J. Wang, and J. Srebric, "Investigating the Impact of Data Normalization Methods on Predicting Electricity Consumption in a Building Using different Artificial Neural Network Models.," *Sustain. Cities Soc.*, vol. 118, no. June 2024, p. 105570, 2024, doi: 10.1016/j.scs.2024.105570.

[15] H. Liu, H. Zeng, and H. Huang, "Bragg resonant re fl ection of surface waves from deep water to shallow water by a fi nite array of trapezoidal bars," *Appl. Ocean Res.*, vol. 94, no. October 2019, p. 101976, 2020, doi: 10.1016/j.apor.2019.101976.